PERGAMON

Aerosol Science 33 (2002) 357–368

Journal of
Aerosol Science

www.elsevier.com/locate/jaerosci

Energy accumulation in nanoparticle collision and coalescence processes

Kari E.J. Lehtinen[a,b,1], Michael R. Zachariah[a,b,*]

[a] *Department of Mechanical Engineering, University of Minnesota, Minneapolis, MN 55455, USA*
[b] *Department of Chemistry, University of Minnesota, Minneapolis, MN 55455, USA*

Received 20 March 2001; received in revised form 23 July 2001; accepted 24 July 2001

Abstract

During coalescence, the surface area of the particle decreases, resulting in a heat release associated with the resulting lower surface energy. In a growth process particle heating competes with heat transfer by conduction to the cooler carrier gas and radiation. This temperature increase can be extremely important and should be accounted for when modeling collision/coalescence processes. The heat release associated with particle coalescence may reduce the coalescence time by as much as a few orders of magnitude. In addition, under some conditions there is insufficient time for the particles to cool to the gas temperature before another collision event takes place. Two such cases are investigated in this paper: (1) low pressure growth of Si nanoparticles and (2) high volume loading growth of TiO_2 nanoparticles. It is shown that accounting for energy release and heat transfer effects have a dramatic effect on primary particle formation and the onset of aggregate formation. The results of the work indicate that to grow the largest primary particles one should operate at low pressures and/or high volume loadings. © 2001 Published by Elsevier Science Ltd.

Keywords: Coalescence; Collision processes; Particle growth

1. Introduction

The ability to predict and control the primary particle size of nanostructured materials is essential since it is a key variable in many thermal, mechanical and optical properties (Ichinose, Ozaki, & Kashu, 1992). Typically in many industrial aerosol processes, a high concentration of very small particles undergoes rapid coagulation. This may lead to the formation of fractal-like agglomerates consisting of a large number of spheroidal primary particles of approximately

* Corresponding author. Tel.: +1-612-626-9081; fax: +1-612-625-6069.
[1] On leave from VTT Energy, Aerosol Technology Group, P.O. Box 1401, 02044 VTT, Finland.
E-mail address: mrz@me.umn.edu (M.R. Zachariah).

0021-8502/01/$ - see front matter
PII: S0021-8502(01)00177-X

uniform diameter (Megaridis & Dobbins, 1990). The size of the primary particles ultimately is determined by the rates of collision and coalescence (Lehtinen, Windeler, & Friedlander, 1996). At high temperatures, coalescence occurs almost on contact resulting in large primary particles and hence small surface area. At low temperatures, the collision rate is faster than the rate of coalescence, leading to fractal-like agglomerates consisting of very small primary particles and thus large surface area. Controlling the coalescence rate is possible through a knowledge of the material properties and the time temperature history of the reactor and the collision rate through the volume loading of the material (Pratsinis, 1998).

Ulrich and Subramanian (1977) first described simultaneous collision and coalescence of agglomerates in flames by assuming that agglomerates consist of a large number of primary particles and treating collision and coalescence as separable processes. Koch and Friedlander (1990) assumed that the coalescence rate of an agglomerate is directly proportional to its excess surface area (actual surface area – equivalent spherical area). This was later shown by Friedlander and Wu (1994) to be exact for the final stages of transformation to sphericity for an originally slightly non-spherical particle. This simple linear decay law for the agglomerate surface area, when combined with a method for solution of the aerosol dynamic equation (GDE), has resulted in several successful models for particle size prediction (Xiong & Pratsinis, 1993; Kruis, Kusters, Pratsinis, & Scarlett, 1993; Windeler, Friedlander, & Lehtinen, 1997; Shimada, Seto, & Okuyama, 1994; Johannesen, 1999). However, in some cases, particularly those that predict very small primary particles of only a few nanometers, these models seem to break down (e.g. Wu, Windeler, Steiner, Bors, and Friedlander (1993) and Windeler et al. (1997), for alumina and Ehrman, Friedlander, and Zachariah (1998), for silica) and underpredict the primary particle size. Recently, Xing and Rosner (1999) used a curvature dependent activation energy for the solid state diffusion coefficient—succeeding in predicting some experimental results for alumina and titania nanoparticle formation. A similar approach was suggested by Tsantilis, Briesen, and Pratsinis (2001) for the viscous flow sintering of silica particles.

Zachariah and Carrier (1999) studied the coalescence of silicon nanoparticles using molecular dynamics (MD) simulation methods. They found that when two particles coalesce, there is a significant increase in particle temperature. This is illustrated in Fig. 1, in which particle temperature vs. time is shown for a typical coalescence event. Following collision the formation of new chemical bonds between the particles results in heat release and the formation of a neck between the particles. This heat release increases the particle temperature rapidly and thus also speeds up the coalescence. An oval shape is formed, which then finally evolves into a sphere.

This effect was studied in detail in our recent paper (Lehtinen & Zachariah, 2001). It was shown that since these particles coalesce by the mechanism of solid state diffusion which is an extremely sensitive function of temperature, the temperature increase within the particle has an important effect to the dynamics of coalescence. In fact, it was shown that for Si nanoparticle coalescence, the effect reduced in some cases the coalescence time by 1–2 orders of magnitude and that heat transfer rate played a critical role. Below a critical gas temperature, all the generated heat release is conducted to the surrounding gas, whereas above the critical temperature a sharp increase in particle temperature is observed, and with it a significant reduction in coalescence time.

In this paper, we proceed a little further, with an idea illustrated in Fig. 2. In some cases, we expect the collision time, τ_c to be short enough that after the particle temperature increase

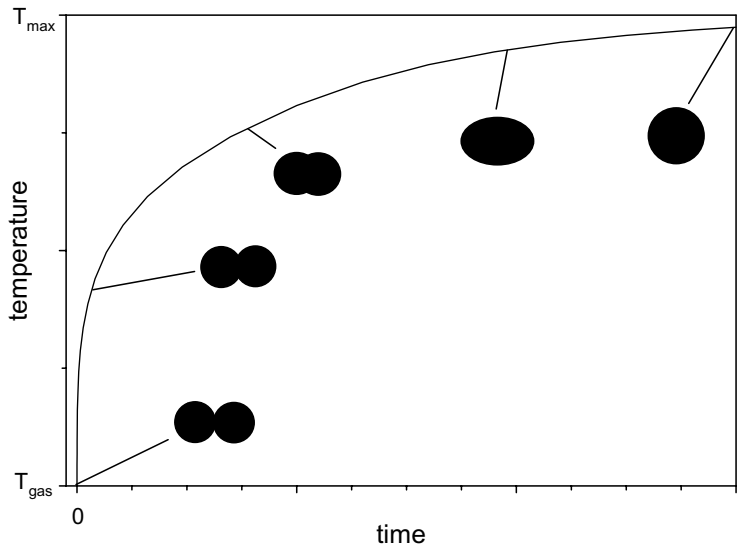

Fig. 1. The evolution of particle temperature and shape in nanoparticle coalescence. The decreasing surface area results in an energy release and, thus, an increase in temperature.

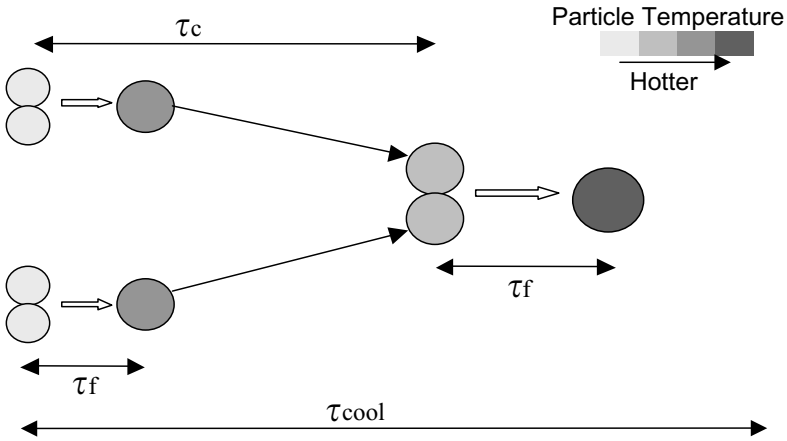

Fig. 2. Collision, coalescence and cooling at early stages of particle growth. Particles coalesce as they collide, i.e. collision time τ_c is larger than coalescence (fusion) time τ_f. Coalescence is accompanied by heating, and cooling due to conduction or radiation is slow, i.e. the cooling time τ_{cool} is large.

due to coalescence, there is not enough time for the particle to cool (τ_{cool}) to gas temperature before a new collision event occurs ($\tau_c < \tau_{cool}$). It is thus possible that successive collision/coalescence events increase the particle temperature much above the gas temperature, thus affecting coalescence times even more. We will show that this can be important for at least two important cases, (a) low pressure growth processes and (b) high volume loading conditions.

2. Theory

Let us consider a system consisting of two identical spherical particles each with N atoms or units (e.g. TiO_2 one unit consists of one Ti atom and two O atoms). During coalescence, a neck rapidly forms between the particles, which transforms into a spherule, and slowly approaches a sphere (see Fig. 1 of this paper or Fig. 3 of Zachariah and Carrier (1999)). We assume that the energy E of our system throughout the coalescence process can be described with bulk and surface contribution terms (Zachariah, Carrier, & Blasiten-Barojas, 1996):

$$\begin{array}{ll} & E_{\text{bulk}} \qquad\quad +E_{\text{surf}} \\ E = & 2N\lfloor \varepsilon_{\text{b}}(0) + c_v T_{\text{p}} \rfloor \; +\sigma a, \end{array} \tag{1}$$

where a is the surface area of the coalescing pair of particles, σ the surface tension, $\varepsilon_{\text{b}}(0)$ the bulk binding energy (negative) at zero temperature and c_v the constant volume heat capacity. All variables are expressed in SI units throughout this work. Any change in total energy of the particle can only result from energy loss to the surroundings, either by convection/conduction to the gas or radiation:

$$\frac{\mathrm{d}E}{\mathrm{d}t} = 2Nc_v\frac{\mathrm{d}T_{\text{p}}}{\mathrm{d}t} + \sigma\frac{\mathrm{d}a}{\mathrm{d}t} = -Zc_{\text{g}}a_{\text{sph}}(T_{\text{p}} - T) - \varepsilon\sigma_{\text{SB}}a_{\text{sph}}(T_{\text{p}}^4 - T^4). \tag{2}$$

Here T is the gas temperature and c_{g} the heat capacity of gas molecules. The emissivity of the particles is ε and σ_{SB} is the Stefan–Boltzmann constant. By rearranging and assuming that the surface area reduction can be approximated by the well-known linear rate law developed by Koch and Friedlander (1990),

$$\frac{\mathrm{d}a}{\mathrm{d}t} = -\frac{1}{\tau_{\text{f}}}(a - a_{\text{sph}}), \tag{3}$$

we get an equation for the particle temperature as

$$2c_vN\frac{\mathrm{d}T_{\text{p}}}{\mathrm{d}t} = \frac{\sigma}{\tau_{\text{f}}}(a - a_{\text{sph}}) - Zc_{\text{g}}a_{\text{sph}}(T_{\text{p}} - T) - \varepsilon\sigma_{\text{SB}}a_{\text{sph}}(T_{\text{p}}^4 - T^4), \tag{4}$$

where the characteristic coalescence, or fusion time (for volume diffusion) is

$$\tau_{\text{f}} = \frac{3kTN}{64\pi\sigma D} \tag{5}$$

and

$$Z = \frac{p}{\sqrt{2\pi m_{\text{g}}kT}} \tag{6}$$

is the collision rate of the free molecular particle with gas molecules (of mass m_{g}), obtained from kinetic gas theory.

The first term on the r.h.s. of Eq. (4) is the heat increase due to coalescence. The remaining terms are the heat loss due to collisions with gas molecules and radiation, respectively (Williams & Loyalka, 1991). The collision rate of gas molecules with the free molecular particle Za is assumed to equal Za_{sph}, and thus unaffected by the coalescence shape evolution.

As discussed in the introduction, the coalescence process reduces the surface area and hence also the surface energy of the particles. There is a competition for this energy—some of it

increases the particle temperature, the rest is conducted or radiated away. A detailed description of the coalescence dynamics and heat transfer is obtained by solving Eqs. (3) and (4). The non-dimensionalization and numerical solution of Eqs. (3) and (4) are explained in detail in Lehtinen and Zachariah (2001) and will be omitted here.

It is noteworthy that Eq. (4) is very non-linear and sensitive to the conditions. The sensitivity to temperature comes from the exponential dependence of the diffusion coefficient D on temperature:

$$D = A \exp\left(-\frac{B}{T_p}\right). \tag{7}$$

If the gas temperature is high enough, the particle temperature increase due to heat release from coalescence will be faster than the heat transferred to the surroundings. This will increase the diffusion coefficient and, hence, the coalescence rate—which will increase the temperature, and so on. If the gas temperature is low, conduction and radiation will dominate, and thus the particle temperature will always stay at the gas temperature.

3. Results and discussion

3.1. Temperature increase during coalescence

In our previous work (Lehtinen & Zachariah, 2001) we compared our method with molecular dynamics (MD) simulations by Zachariah and Carrier (1999), i.e. simulated the coalescence of silicon nanoparticles of size $N = 30, 60, 120$ and 240 for gas temperature $T = 600$ K. Both the maximum temperature increase of the coalescing particle as well as the coalescence time agreed reasonably well with the MD results. In addition, it was found that there is a sharp boundary in conditions, for which this temperature increase becomes important. The material properties for Si in this work were chosen to be the same as in Lehtinen and Zachariah (2001) and Zachariah et al. (1996).

To explain this effect more clearly, some of the results are reproduced here as Figs. 3(a) and (b). In Fig. 3(a), the coalescence event is studied for two Si nanoparticles with $N = 1000$ atoms each. The dashed line corresponds to a calculation in which the heat release due to coalescence has been neglected. The solid line and dotted line are the excess surface area and the particle temperature from the numerical solution to Eqs. (3) and (4), i.e. the heat release and gas cooling are accounted for. In this case, the coalescence is sufficiently fast so that heat conduction to the surrounding gas is negligible, as evidenced by the flat temperature profile during the neck growth process.

In Fig. 3(b), we plot the coalescence time as a function of gas temperature. One can see that there exists a temperature at which there is a sudden change in the dynamics of Eq. (4) and therefore the coalescence rate. Below the critical temperature, particle heating is negligible and the coalescence time is long. Then, over a very narrow temperature window at around 318 K the coalescence time drops two orders of magnitude. This clearly illustrates the non-linear nature of the competing heat generation/extraction terms. If a critical temperature increase is exceeded, it increases the coalescence rate exponentially, which correspondingly speeds up the temperature

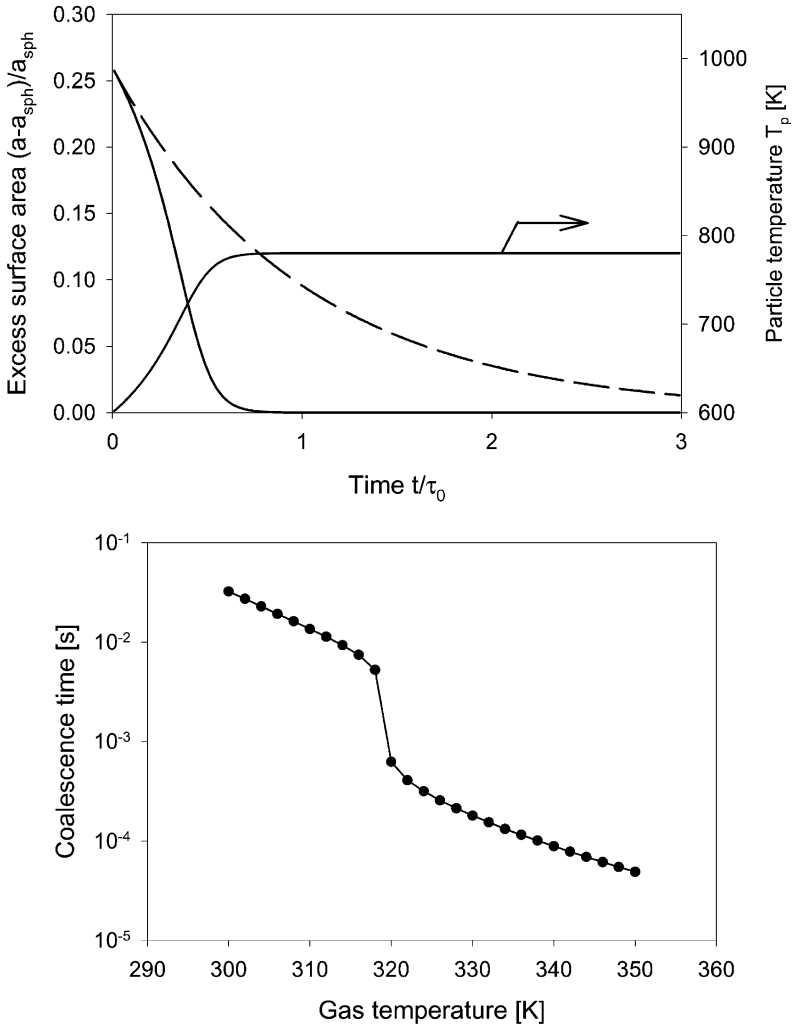

Fig. 3. Effect of heat release on the coalescence of Si nanoparticles of size 1000 atoms (3.4 nm) in air. (a) The evolution of surface area (solid black line) and temperature (solid gray line) at $T_g = 600$ K. The dashed line is the surface area evolution if coalescence heat release is neglected. τ_0 is the coalescence time if heat release is neglected. (b) The coalescence time as a function of gas temperature.

increase rate and so on. If this critical temperature is not exceeded, coalescence is slow and the heat release energy is conducted or radiated to the surrounding gas.

3.2. Energy accumulation during high volume loading coagulation

We now extend the analysis to include coagulation and look at an interesting example—coagulation in a system with a high aerosol volume loading, a condition of particular relevance to industrial growth conditions. When the volume loading is high, particles coagulate rapidly and

therefore the time between collisions (τ_c) is short. Thus, there is only a short time available for cooling to take place before another collision event. If indeed, conditions are met such that $\tau_c < \tau_{cool}$, then we should expect to see a rising particle temperature. The particle temperatures can in fact rise to levels that phase changes might occur, which means that coalescence dynamics can be changed dramatically. This will be highlighted in the following example: TiO_2 collision/coalescence at $T_g = 1600$ K and $p = 1$ atm.

Initially, let us assume that we have monodisperse particles of diameter ≈ 1 nm and study two cases: (a) volume loading ϕ of these particles is 10^{-3} (industrial conditions) and (b) 10^{-6} (laboratory conditions). The growth of the particle volume can be approximated by the monodisperse growth model (in the free molecular regime, as in Kruis et al. (1993)):

$$\bar{v} = \left(\bar{v}_0^{5/6} + \frac{5}{6}\gamma t\right)^{6/5}, \qquad \gamma = 2.228\left(\frac{6kT}{\rho_p}\right)^{1/2}\phi. \tag{8a,b}$$

This growth law holds for completely coalescing particles. The melting point of nanoparticles T_{mp} can be approximated by (Buffat & Borel, 1976)

$$T_{mp} = T_m\left[1 - \frac{4}{L\rho_s d_p}\left(\sigma_s - \sigma_\ell\left(\frac{\rho_s}{\rho_\ell}\right)^{2/3}\right)\right] \tag{9}$$

in which T_m is the bulk melting point, L the latent heat of melting, σ_s and σ_ℓ the surface tension and ρ_s and ρ_ℓ the densities of solid and liquid, respectively. For titania, we have used (Samsonov, 1982; German, 1996): $T_m = 2103$ K, $L = 600$ kJ/K, $\sigma_s = 0.6$ J/m^2, $\sigma_\ell = 0.34$ J/m^2, $\rho_\ell = \rho_s = 3840$ kg/m^3. This means that particles of diameter 1 nm are liquid at 1600 K, and coalescence is practically instantaneous at contact. The particle temperature will rise as explained in the previous section, and then cool by conduction and radiation when the particle is waiting for a new collision. If the cooling time is short enough, the particle will start its next coalescence event at a higher temperature than T_g, making coalescence faster.

As is inherently assumed in the monodisperse model, we will study the TiO_2 collision/coalescence process assuming all the collisions occur synchronously. This means that all the monomers will coagulate at the same time, then all dimers will do the same, etc. The collision times can be obtained directly by setting $\bar{v} = 2v_0, 4v_0, 8v_0, \ldots$ in Eq. (8) and solving for time. The collision times are presented in Table 1. Then each coalescence event is simulated, using Eqs. (3) and (4), solving for the surface area and temperature of the coalescing particle. The results are presented in Table 1 (for the $\phi = 10^{-3}$ case) and graphically (for both cases) in Figs. 4(a) and (b). The black line in both figures is the particle temperature, the gray lines represent the particle melting temperature for the corresponding size. The sharp jumps in temperature represent the coalescence events, which occur practically instantaneously for the liquid phase nanoparticles. Note that the time axes of both figures are logarithmic and of different scales.

In the industrial loading case ($\phi = 10^{-3}$) something very interesting occurs: the heat release from successive coalescence events keeps the particle temperature above the melting point for a long time, up to the point where the particle temperature and melting temperature curves cross, which corresponds to roughly $d_p = 10$ nm in particle diameter. After this point the coalescence rate becomes very slow—for 10 nm solid TiO_2 particles the coalescence time is milliseconds,

Table 1
Heat accumulation in TiO_2 collision and coalescence; N = number of TiO_2 molecules per particle, d_p = particle diameter, t = time, T_{mp} = melting temperature, T_{max} = maximum temperature, T_{fin} = final temperature

N	d_p (nm)	t (ns)	T_{mp} (K)	T_{max} (K)	T_{fin} (K)
15	0.996	0	1151	1600	1600
30	1.26	1.31	1350	1738	1736
60	1.58	3.65	1503	1846	1843
120	1.99	7.81	1626	1930	1924
240	2.51	15.2	1725	1994	1983
480	3.16	28.5	1803	2039	2022
960	3.99	52.0	1865	2066	2040
1920	5.02	94.0	1914	2076	2039
3840	6.33	169	1953	2067	2018
7680	7.97	302	1984	2041	1977
15,360	10.0	539	2008	1995	1918

compared with the microseconds total simulation time of our example. Furthermore, without taking this temperature increase effect or the melting point reduction into account, Eq. (5) predicts a coalescence time of 4.4 μs for the initial coalescence event of two 1 nm particles coalescing, which roughly equals our total simulation time.

For the laboratory scale case ($\phi = 10^{-6}$) the situation is totally different. The first collision/coalescence event again raises the particle temperature from 1600 to 1738 K, but before the next collision there is sufficient time for the particles to relax to gas temperature again. In this example, as seen in Fig. 4b, we will thus only have three successive collisions in the liquid phase. Thereafter ($d_p > 2$ nm), the particles are solid and the coalescence rate will slow down. There is still coalescence occurring because the time scales are now much longer, but no temperature increases, as seen in Fig. 4b. The collision/coalescence dynamics of the system can thus be modeled using the standard Koch and Friedlander (1990) approach.

3.3. Energy accumulation during low-pressure coagulation

Now, let us look at another case in which heat accumulation can be important—low pressure nanoparticle synthesis. As seen in Eq. (4), the cooling term (by conduction) is proportional to gas pressure. This means that if the pressure is decreased by a factor of 1000, the cooling rate will be decreased by this same factor. Again, it is foreseeable that since the cooling rate is so low, there is not enough time for the particles to relax to the gas temperature between successive collisions.

As an example case, we simulate the growth of Si nanoparticles at $T_g = 50^{\circ}C$, $p = 100$ Pa and with initially $d_p = 1$ nm particles of volume loading $\phi = 10^{-6}$. As in the TiO_2 case, we use the monodisperse model and solve for the collision times from Eq. (8). Then Eqs. (3) and (4) are solved for each coalescence event to obtain the surface area and temperature of the coalescing particle. The results are shown in Fig. 5.

At time $t = 0$, we have individual particles of volume $v_0 (= \pi(1\text{ nm})^3/6)$. At $t = 1.94$ μs the particles collide, form particles of volume $2v_0$, and start to coalesce. During coalescence, the

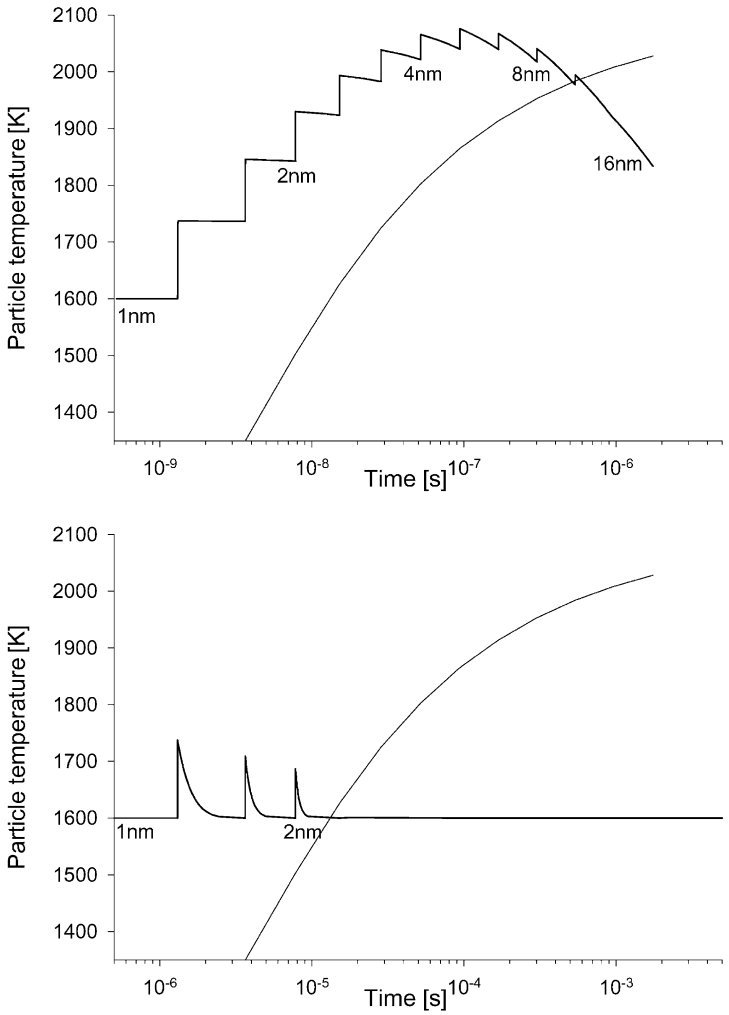

Fig. 4. Collision, coalescence and heat increase of TiO_2 nanoparticles at 1600 K and 1 atm in air with (a) volume loading 10^{-3} (b) volume loading 10^{-6}. The black lines are the particle temperature. Collision and immediate coalescence occurs at the sharp increases of particle temperature. Particle melting temperature is indicated with gray lines.

length of which is indicated with τ_f in Fig. 4, the particle temperature rises to 925 K. Between 1.94 and 5.41 μs, when the particle is waiting for its next collision, the temperature decreases to 790 K because of conduction and radiation. The cooling rate is not sufficient to relax the particle to the gas temperature, which means that the next coalescence event will start at a higher temperature and is, therefore, much faster. This can be seen from Fig. 5 from the sharp temperature rise at $t = 5.41$ μs. The same pattern repeats itself several times, until the time scales become long enough that conduction and radiation have enough time to cool the particle between collisions to near gas temperature. At $v = 512v_0$ ($t = 448$ μs) the coalescence rate drops off dramatically and there is practically no more coalescence.

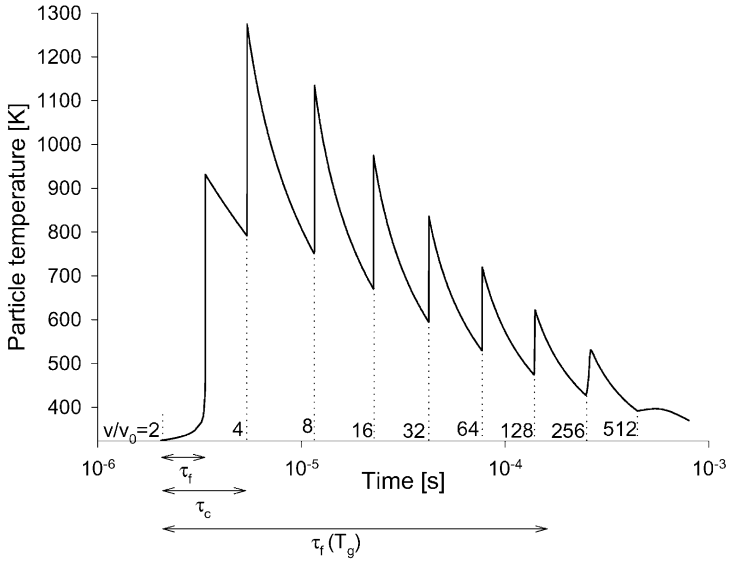

Fig. 5. Collision coalescence and heat increase of Si nanoparticles at $T_g = 50^{\circ}C$ and $p = 100$ Pa in air with an aerosol volume fraction $\phi = 10^{-6}$ and initial particle diameter $d_p = 1$ nm. The numbers right above the time axis indicate the particle volume at the corresponding time. The arrows at the bottom show the characteristic coalescence (τ_f) and collision times (τ_c) of the first collision/coalescence event as well as the coalescence time ($\tau_f(T_g)$) if the heat increase would be neglected.

One of the dramatic effects of taking into account the heat release is the comparison of coalescence times at the bottom of Fig. 5. As already explained, the coalescence time of the first coalescence event (taking the heat release properly into account) is indicated by τ_f. This is shorter than the collision time τ_c so the particles have time to fully coalesce before the next collision. However, if the heat release were not accounted for then the coalescence time would be calculated at the gas temperature (from Eq. (5)), and one would predict a coalescence time two orders of magnitude higher (see Fig. 5). This would mean an onset of aggregation occurring immediately, and a primary particle size that of the monomer!

4. Conclusions

In this paper, we have continued our analysis of the thermal behavior of coalescing nanoparticles resulting from heat release in collision/coalescence processes. The transformation of two spherical nanoparticles into one completely fused one is a process driven by minimizing the surface free energy and is reflected in a temperature increase of the resulting particle. Since the characteristic coalescence time is inversely proportional to the solid state diffusion coefficient, which is very sensitive (exponentially dependent) to temperature, under certain circumstances the heat release associated with the initial stages of coalescence can significantly impact the overall coalescence process. In a previous study, we have used the simple exponential decay law for the excess surface area of the coalescing particles, and modified it in such a way

that particle temperature and hence also the characteristic coalescence time are time dependent variables. In this paper, we have extended this approach by including coagulation to our model. If the collision time is short enough, there is insufficient time for the particles to relax to the gas temperature before another collision event takes place and the resulting coalescence rates are increased even further.

The effect of energy accumulation during coagulation is important in cases with long cooling times, compared with collision times. Two such systems are investigated: Si low pressure and TiO_2 high volume loading nanoparticle growth. Since the cooling rate by conduction is proportional to gas pressure, at low pressures conduction is too slow a mechanism to cool particles to gas temperature between collision events. The same thing happens for high volume loading cases when the collision time is too short for cooling to take place. The high volume loading case is highly relevant in that most industrial bulk scale production of nanoparticles (e.g. TiO_2 pigment production) occur at very high volume loadings. Indeed the results suggest that laboratory based experiments which are typically conducted at low volume loading may be entirely off the mark if the goal is to understand how to grow nanoparticles under industrial conditions.

For both, Si nanoparticle growth at low pressure and TiO_2 at high volume loading cases, we see that energy accumulation/transfer play a critical role. In the Si case, neglecting energetic effects would mean that using the well-known Koch and Friedlander model would result in aggregate formation at monomer scale. Taking the heat increase into account enables particles to grow to 1000 times their initial volume. For TiO_2, we compared industrial conditions (volume loading $= 10^{-3}$) with laboratory conditions (10^{-6}). Under laboratory conditions, the primary particles grew to only 2 nm, compared with 10 nm at industrial conditions. In the low volume loading case, the time between collisions is long enough for relaxation to gas temperature. For high volume loadings, the particle temperature can rise up to 500 K above the gas temperature, causing a phase change from solid to liquid, where nanoparticles coalesce practically instantaneously.

Finally, one of the primary conclusions from this work. If you want to grow large primary particles without using excessively high gas temperatures—*use very high loadings and/or low pressures*.

References

Buffat, P., & Borel, J. P. (1976). *Physical Review A*, *13*, 2287.

Ehrman, S. H., Friedlander, S. K., & Zachariah, M. R. (1998). *Journal of Aerosol Science*, *29*, 687.

Friedlander, S. K., & Wu, M. K. (1994). *Physics Review B*, *49*, 3622.

German, R. M. (1996). *Sintering theory and practice*. New York: Wiley.

Ichinose, N., Ozaki, Y., & Kashu, S. (1992). *Superfine particle technology*. Berlin: Springer.

Johannesen, T. (1999). *Synthesis of nano-particles in flames*. Ph.D. thesis, TU Denmark.

Koch, W., & Friedlander, S. K. (1990). *Journal of Colloid Interface Science*, *140*, 419.

Kruis, F. E., Kusters, K. A., Pratsinis, S. E., & Scarlett, B. (1993). *Aerosol Science and Technology*, *19*, 514.

Lehtinen, K. E. J., Windeler, R. S., & Friedlander, S. K. (1996). *Journal of Aerosol Science*, *27*, 883.

Lehtinen, K. E. J., & Zachariah, M. R. (2001). Energy accumulation during the coalescence and coagulation of nanoparticles. *Physical Review B, 63*(20), 205402/1–205402/7.

Megaridis, C. M., & Dobbins, R. A. (1990). Morphological description of flame-generated materials. *Combustion Science and Technology*, *71*, 95.

Pratsinis, S. E. (1998). Flame aerosol synthesis of ceramic powders. *Progress in Energy and Combustion Science*, *24*, 197.

Samsonov, G. V. (1982). *The oxide handbook*. New York: IFI/Plenum.

Shimada, M., Seto, T., & Okuyama, K. (1994). Size change of very fine silver agglomerates by sintering in a heated flow. *Journal of Chemical Engineering Japan*, *27*, 795.

Ulrich, G. D., & Subramanian, N. S. (1977). Particle growth in flames III: coalescence as a rate controlling process. *Combustion Science and Technology*, *17*, 119.

Tsantilis, S., Briesen, H., & Pratsinis, S. E. (2001). Sintering time for silica particle growth. *Aerosol Science and Technology*, *34*, 237.

Williams, M. M. R., & Loyalka, S. K. (1991). *Aerosol science: Theory and practice*. Oxford: Pergamon Press.

Windeler, R. S., Friedlander, S. K., & Lehtinen, K. E. J. (1997). Production of nanometer-sized metal oxide particles by gas phase reaction in a free jet. *Aerosol Science and Technology*, *27*, 191.

Wu, M. K., Windeler, R. S., Steiner, C. K. R., Bors, T., & Friedlander, S. K. (1993). Controlled synthesis of nanosized particles by aerosol processes. *Aerosol Science and Technology*, *19*, 527.

Xing, Y., & Rosner, D. E. (1999). Prediction of spherule size in gas phase nanoparticle synthesis. *Journal of Nanoparticle Research*, *00*, 1.

Xiong, Y., & Pratsinis, S. E. (1993). Formation of irregular particles by coagulation and sintering. *Journal of Aerosol Science*, *24*, 283.

Zachariah, M. R., Carrier, M. J., & Blasiten-Barojas, E. (1996). Properties of silicon nanoparticles: a molecular dynamics study. *Journal of Physical Chemistry*, *100*, 14,856.

Zachariah, M. R., & Carrier, M. J. (1999). Molecular dynamics computation of nanoparticle sintering: comparison with phenomenological models. *Journal of Aerosol Science*, *30*, 1139.